Cosmic Research, Vol. 40, No. 1, 2002, pp. 1–14. Translated from Kosmicheskie Issledovaniya, Vol. 40, No. 1, 2002, pp. 3–16.

Statistical Relationships between Solar, Interplanetary, and Geomagnetospheric Disturbances, 1976–2000

Yu. I. Yermolaev and M. Yu. Yermolaev

Space Research Institute, Russian Academy of Sciences, Profsoyuznaya 84/32, Moscow 117997, Russia

Received May 31, 2001

Abstract—Within the framework of the Space Weather program, 25-year data sets for solar X-ray observations, measurements of plasma and magnetic field parameters in the solar wind, and D_{st} index variations are analyzed to reveal the factors that have had the greatest influence on the development of magnetospheric storms. The correlation between solar flares and magnetic storms practically does not exceed a level of correlation for random processes. In particular, no relation was found between the importance of solar flares and the minimum of the D_{st} index for storms that could be connected with considered flares by their time delay. The coronal mass ejections (CME; data on these phenomena cover a small part of the interval) result in storms with $D_{st} < -60$ nT only in half of the cases. The most geoeffective interplanetary phenomena are the magnetic clouds (MC), which many believe to be interplanetary manifestations of CMEs, and compressions in the region of interaction of slow and fast streams in the solar wind (the so-called Corotating Interaction Region, CIR). They correspond to about two-thirds of all observed magnetic storms. For storms with $-100 < D_{st} < -60$ nT, the frequencies of storms from MC and CIR being approximately equal. For strong storms with $D_{st} < -100$ nT, the fraction of storms from MC is considerably higher. The problems of reliable prediction of geomagnetic disturbances from observations of the Sun and conditions in interplanetary space are discussed.

INTRODUCTION

One of the key problems of solar–terrestrial physics in general and of the Space Weather program in particular is the problem of revealing the solar and interplanetary factors that cause magnetospheric disturbances. Knowing these factors, models can be constructed that allow predictions to be made of conditions in near-Earth space and the magnetosphere on the basis of observations of the Sun and interplanetary medium. Although this problem has been investigated for a long time and there is now a large body of experimental and theoretical results (see, for example, the collection of papers [1] and reviews [2–4]), the problem is far from being solved.

By and large, the concept describing the connection of geomagnetic phenomena with processes on the Sun can be presented as follows. The source of energy for geomagnetic phenomena is the Sun, which transfers energy to the Earth's magnetosphere by the solar wind (SW). The SW energy arrives in the magnetosphere only when the interplanetary magnetic field (IMF) has a significant component parallel to the terrestrial magnetic dipole, i.e., it has an approximately negative (southward) IMF B_z component (see, for example, [5] and references therein). When the rate of energy input is higher than the rate of its quasistationary dissipation, energy is accumulated in the magnetosphere. When it reaches and exceeds a certain level, any small disturbance outside or inside the magnetosphere can result in the release of this energy (a so-called trigger mechanism), which is observed as a reconnection of magnetic field lines, global reorganization of current systems in the magnetosphere, and heating/acceleration of plasma, i.e., a magnetospheric disturbance can be generated.

Quasistationary SW usually does not contain long intervals of southward components of IMF since the field basically lies in the ecliptic plane. However, sometimes large-scale disturbances propagate in the SW, such as interplanetary shocks (IS), magnetic clouds (MC), regions of compression on the boundary of slow and fast streams (corotating interaction regions, CIR), and some other disturbances. They either contain an appreciable southward IMF B_z component within or they modify the environment in such a manner that this component can be present in the SW for several hours. Such behavior of the IMF can result in energy input into the magnetosphere and in generation of magnetospheric disturbances (see [3, 4, 6, 7]). We emphasize that the term "corotating interaction region," which has a long history in the literature, is very inadequate in our opinion, because not all CIR are corotating (repeating with the period of the Sun's rotation). It would be more appropriate to call them "stream interaction regions (SIR)," but we will follow tradition and use the conventional term.

Historically, of all active processes on the Sun, the solar flares were discovered first, and for a long time all disturbances in the SW and the Earth's magnetosphere were associated exclusively with solar flares. For exam-

0010-9525/02/4001-0001$27.00

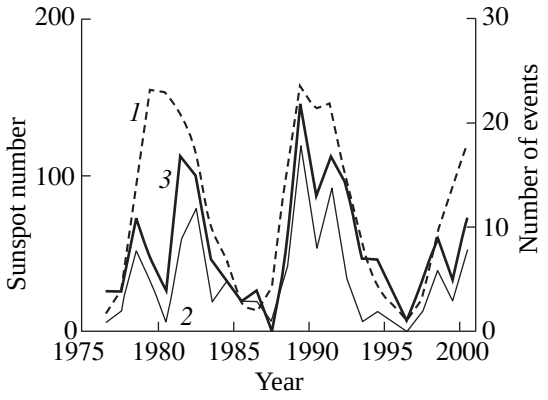

Fig. 1. Time variations of yearly averaged values of the sunspot number (curve *1*, scale on the left), the number of strong (importance of M and X) solar flares (curve *2*, scale on the right), and the number of strong magnetic storms with minimum values of the D_{st} index lower than –60 nT (curve *3*, scale on the right).

ple, in the book *Physics of Space: A Small Encyclopedia* (1986) the article on solar–terrestrial links [8] mentioned only flares. After the discovery of another powerful solar process, coronal mass ejections (CME), in the beginning of the 1970s, CMEs have been studied only by separate researchers and, on the whole, were almost not used in considering the chain of solar–terrestrial relations. However, after the famous paper by Gosling [9], this has changed, and now CMEs are considered almost as a unique cause of all interplanetary and geomagnetic disturbances [2, 4, 10].

In this paper, we use long-term observations of the Sun, interplanetary space, and the geomagnetic D_{st} index to study the geoefficiency of solar and interplanetary phenomena, i.e., their ability to generate magnetic storms on the Earth. We also discuss some aspects of forecasting geomagnetic disturbances on the basis of solar and interplanetary observations.

1. DESCRIPTION OF DATA AND GENERAL CHARACTERISTICS OF THE PERIOD

For our analysis, we used the following data available on the Internet: a list of strong solar flares of classes (in the X-ray range) from M0 and higher (http://sec.noaa.gov/ftpdir/indices/SPE.txt); three parameters of solar wind plasma (velocity, temperature, and density of ions), the magnitude and three components of the IMF (http://nssdc.gsfc.nasa.gov/); as well as hourly averaged values (not corrected) of the D_{st} index (http://nssdc.gsfc.nasa.gov/ and http://swdcdb.kugi.kyoto-u.ac.jp/dstdir/) from 1976 to 2000. It is necessary to note that if the measurements of X-ray emission of solar corona and terrestrial D_{st} index cover practically 100% of the interval, the data sets on the interplanetary medium before launching of the *Wind* (1994) and *ACE* (1997) spacecraft have significant data gaps, and the time resolution of the early data was equal to 1 h. We did not find regular catalogs of CME events and, consequently, we had to restrict ourselves to a discussion of the published results on CME observations.

Here, we must make one serious comment concerning the data used in other studies. Many researchers use SW and IMF measurements instead of direct CME observations of the solar corona. As was shown by the analysis carried out earlier, the SW and IMF parameters, measured 2–4 days after the CME observations in the corona, have features that are close to those characteristic of the phenomena referred to as magnetic clouds (MC, see [11, 12]). Although the CME–MC correlation is high enough, the questions of whether a CME always results in an MC and whether an MC can be caused by other solar sources remain unclear. Nevertheless, an MC is frequently referred to as a CME, and conclusions are drawn on CME relationships, although they were actually found for MCs. As an example of this approach, we can indicate paper [9], mentioned above. As was discovered earlier [6], in the MC observed after detecting CME in the corona, bidirectional electron streams (or counterstreaming halo electrons, CSHE) are found rather frequently. The presence of CSHE usually means that both CME and MC have a magnetic field in the shape of a loop or a closed spiral. Gosling took advantage of this result and all CSHE intervals for the 50-month period under study were considered as CME intervals. The dependences obtained in this case concern only CSHE, and it is not known how many of them are really connected to CME. We agree that the use of additional information on the SW stream (such as CSHE, helium enhancement, unusual ionization states of heavy ions, etc.) allows one to identify the types of SW streams more precisely and to establish a stricter relationship between MC streams and CMEs. However, in our opinion, to speak about this relationship now is premature [13]. As will be shown below, based on measurements in interplanetary space, we have selected some types of SW (including MC). However, their connection with phenomena such as CME can only be considered a hypothesis.

The general situation in the 25-year period under consideration is characterized in Fig. 1, where the dashed line (curve *1*) shows the yearly-averaged sunspot number, the thin line (curve *2*) gives the number of strong solar flares with an importance no lower than M0, and the thick line (curve *3*) represents the number of strong magnetic storms (see definition below). The period began with a solar cycle minimum in 1976. Then, there were two full cycles of solar activity, and the twenty-third cycle started in 1996, which reached its maximum in 2000. The numbers of strong flares and strong storms were maximal simultaneously with sunspot maxima. Attention is drawn to the fact that curves *2* and *3* have very similar shapes (the correlation coefficient is 0.92), and this correlation is indicative of a common cause of the variations of these two parameters. However, as will be shown below, magnetic storms turn out to be practically unrelated to solar flares.

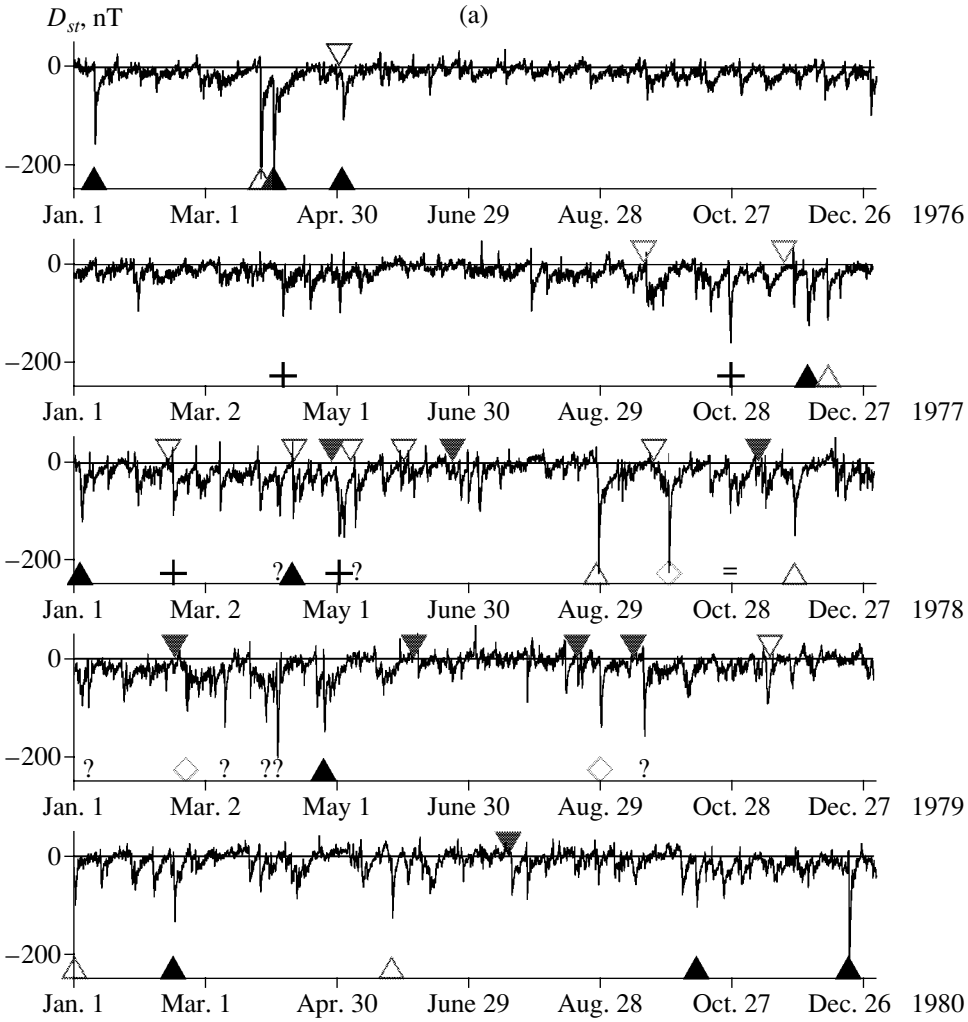

Fig. 2. Time variations of hourly averaged values of the D_{st} index (continuous line), strong solar flares (top triangles: open and solid and correspond to the western and eastern flares), and phenomena in the interplanetary space (bottom symbols: solid triangles represent MC, open triangles correspond to CIR, diamonds to IS, question mark means unclear event, and cross stands for no data available).

2. STATE OF THE MAGNETOSPHERE

We use measurements of the D_{st} index (see the solid line in Fig. 2) as an indicator of geomagnetic activity. This index is basically connected to the geomagnetic field near the equator and to the condition of the ring current, and it describes the development of global large-scale geomagnetic disturbances (magnetic storms) well. We used the original data on the D_{st} index without taking into account the contribution of currents on the magnetopause surface to the D_{st} index value. In quiet times, the D_{st} index varies near zero, slightly changing in the range from –30 up to + 30 nT. The magnetic storm is usually accompanied by a sharp (1–10 h) drop of the D_{st} index down to a minimum value and by slow (1–3 days) recovery of the D_{st} index up to an initial value near zero.

In Fig. 3, the distributions of hourly averaged values of the D_{st} index for the entire period from 1976 to 2000 (thick line, scale to the right) are shown, as well as the same distributions for the disturbed year (1989; thin solid line) and quiet year (1976; dashed line). The scales are adjusted in such a manner that all three distributions have approximately identical areas. All distributions have a bell-like part in the range from –30 up to + 20 nT, which includes the majority of measurements. However, on all distributions (and especially for the disturbed year) there are tails in the region of negative values of the D_{st} index. Decreases lower than –30 nT are usually referred to as magnetic storms. Although there are no conventional techniques and terminology for the classification of magnetic storms in the literature, we accept the frequently used scale and consider storms with a D_{st} index from –30 to –60 nT as weak, from –60 to –100 nT as moderate, and those less than –100 nT as

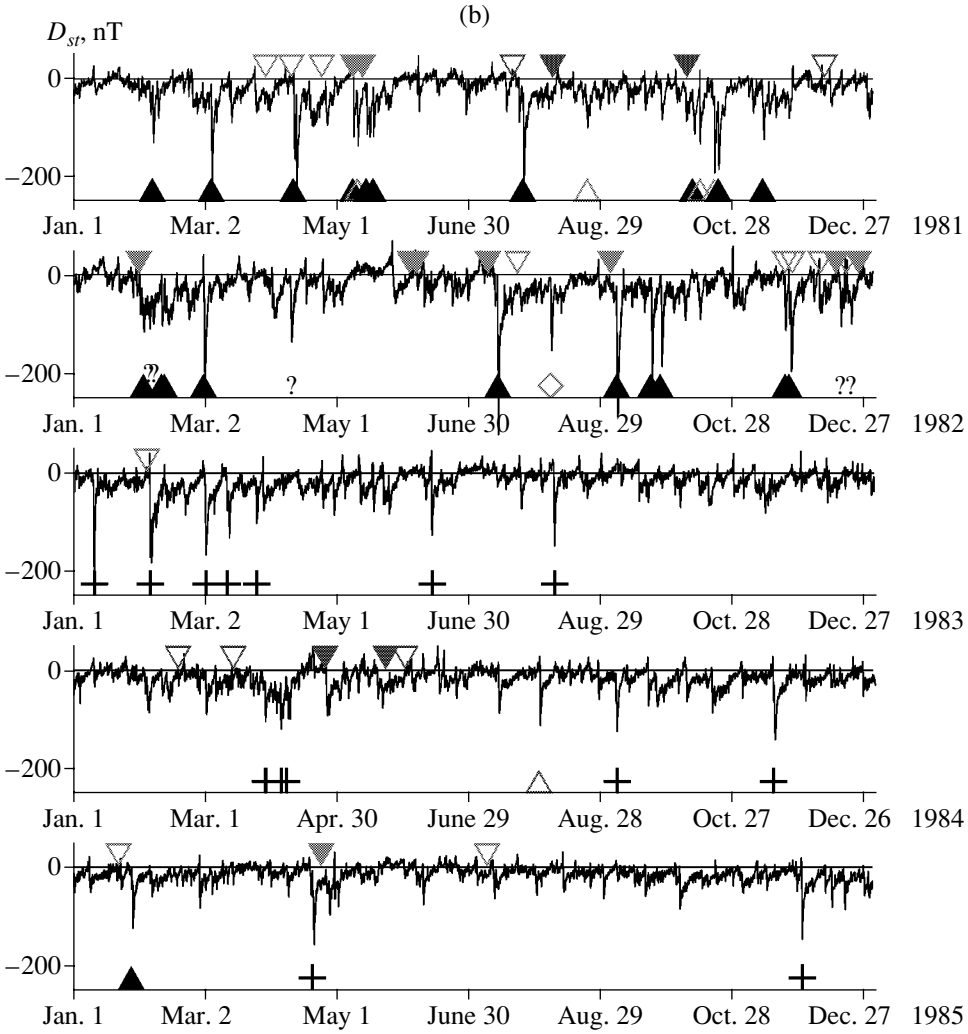

Fig. 2. (Contd.).

strong. Weak storms are too numerous to be considered as isolated from each other: being observed in time close to each other, they can also overlap. This strongly complicates (and in some cases makes impossible) the analysis of their relation to the phenomena on the Sun, because the time of SW motion from the Sun to the Earth is from 2 to 4 days. Therefore, we excluded weak storms from the analysis and restricted ourselves to only moderate and strong storms whose total number was 618 (414 moderate and 204 strong). Thus, on average for the entire 25-year period, a strong or moderate magnetic storm is observed once every ~15 days. In quiet years, this period can increase up to ~45 days, and in disturbed years it can decrease down to ~6.8 days. The strongest magnetic storm for the 25-year period was observed on March 14, 1989, with a peak value of the D_{st} index as low as –589 nT (for this storm, in Fig. 2 we cut off this value at –300 nT).

In addition to variations in the solar activity cycle (see Fig. 1), the number of storms also varies within one year. The number of strong (dash-dotted line) and the total number of moderate and strong (dashed line) magnetic storms were determined for each month by the method of epoch superposition and are shown in Fig. 4. A similar dependence for the number of strong solar flares is presented in the same figure and will be discussed in the next section. Irrespective of the level of magnetic storms, the number of storms has two maxima in spring and in autumn. This result confirms the Russell–McPherron effect [14], which can be connected with annual evolution of the geomagnetic dipole orientation relative to the Sun–Earth line. In particular, such an explanation of this effect is correct under the assumption that the SW energy input into the magnetosphere is possible not only with the existence of the IMF component parallel to the dipole, but also when this component is perpendicular to the incident SW stream. In this case, with a deviation of the Earth's rotation axis perpendicular to the Sun–Earth line in the spring and autumn months (near equinox days), the

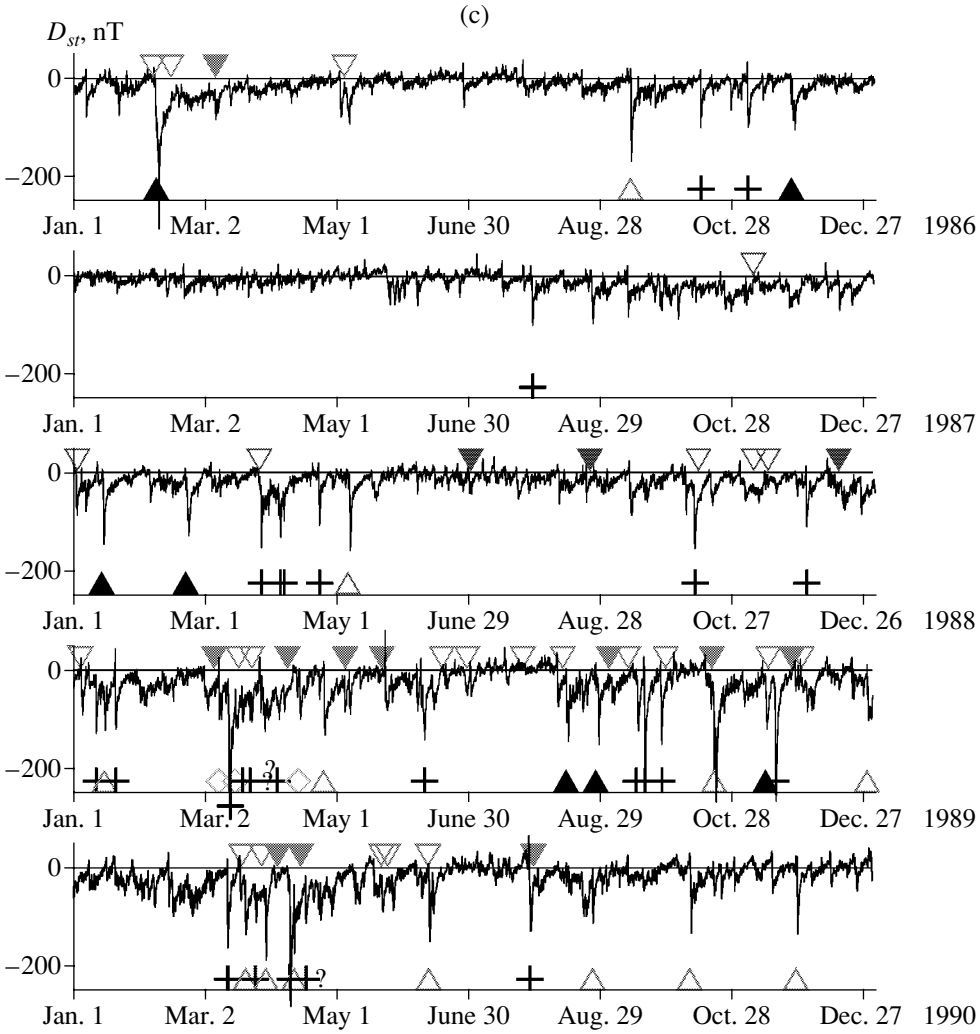

Fig. 2. (Contd.).

IMF B_y component can make an additional contribution to the IMF component parallel to the Earth's magnetic dipole. If one turns from the solar-ecliptic (GSE) system of coordinates to the solar-magnetic (GSM) system, in which the magnetic dipole of the Earth always lies in the XZ plane, the change of direction of the dipole will be taken into account automatically. In what follows, we use the GSM system of coordinates.

3. RELATIONS OF STORMS WITH SOLAR SOURCES

We begin studying the relations between magnetic storms and their solar sources with the analysis of solar flares. The catalog of strong flares is given in the table, where the date and time of a flare, its importance according to X-ray and optical observations, its coordinates and the region number on the Sun, are given. In addition, we have included some extra information on SW types to this catalog. This information will be described below, as well as the method of collection. If the type of interplanetary disturbance is identified (the main types were MC, CIR, and IS), this type of disturbance and the date and time of its beginning are indicated, as well as the minimum of the observed D_{st} index. If the type of interplanetary disturbance is not determined or there are no data for the appropriate interval, then the date and time of a D_{st} minimum are given in the table. The flares for which no magnetic storm was found in the given time interval (see below) have no data given for the D_{st} index and SW type. We have excluded those flares from the analysis whose importance was lower than M0. The same was done with the flares for which there was no information on the time of their beginning, or a previous flare that was separated in time by less than 2 days. In this manner, we obtained a list of 126 strong solar flares.

Although the data on solar flares shown in Fig. 4 have rather small statistical values, we can assume that the distributions of the number of storms and number of

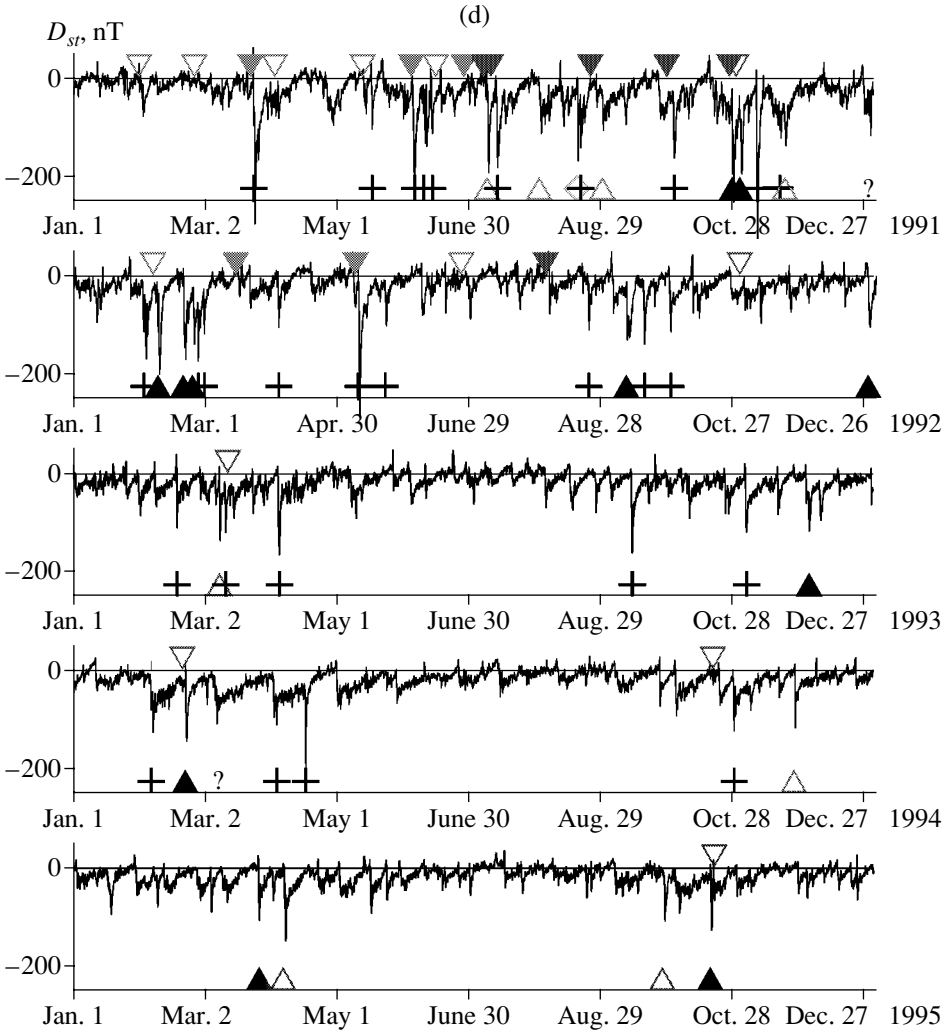

Fig. 2. (Contd.).

strong flares have extreme values in different months of a year. If the two-peak distribution of the number of storms is explained well by the Russell–McPherron effect [14] (see the previous section), the two-peak distribution of the number of flares (and in general their correlation with the period of motion of the Earth around the Sun) is quite unexpected. This is probably connected to the observation selection: the absence of observations of the Sun in winter and summer months. Nevertheless, the figure shows that there is no correlation of flares and magnetic storms on scales less than one year.

In addition to the hourly averaged values of the D_{st} index presented in Fig. 2 by a continuous line, strong solar flares are indicated by triangles in the upper part of each panel, the open and solid triangles correspond to flares on the western and eastern parts of the solar disk, respectively. The figure shows that a great number of storms (strong storms included) have no corresponding flares and many flares are observed far from storms either before or after them. We have correlated all flares with storms using the following algorithm: if a disturbance in the SW (or a minimum of the D_{st} index if the SW disturbance type could not be determined) was observed 2–4 days after a flare, this flare was considered as a potential (most probable) candidate for a solar source of this storm; a flare was considered probable if it fell into the expanded interval of 1.5–5 days; flares in the interval of 1–6 days were considered unlikely; and beyond this interval, they were considered improbable candidates. It is worthwhile to note that the time interval of 2–4 days corresponds to the average propagation velocity of disturbances 430–870 km/s on the Sun–Earth line, which agrees with the usual SW velocity at the Earth's orbit. The results of this analysis are shown as histograms in the upper panel of Fig. 5, and the western and eastern flares are represented by dashed and solid lines, respectively. Histograms *a*, *b*, *c*, and *d* represent, respectively, the most probable sources (25.4%) of storms, probable (18.3%), unlikely (19.0%), and

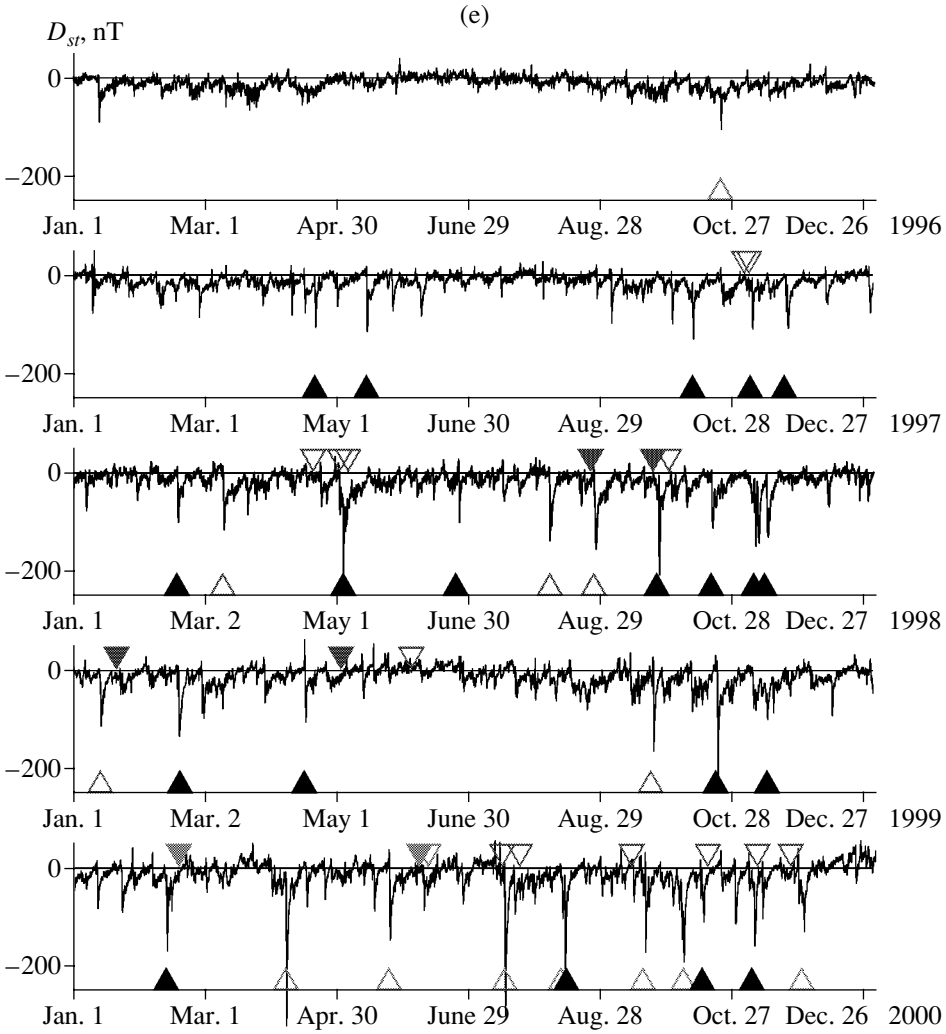

Fig. 2. (Contd.).

improbable (37.3%) sources. As seen from the table, distributions of flares of all types *a*, *b*, *c*, and *d* on the solar disk practically do not differ, and flares of all types are observed in wide ranges of solar latitudes and longitudes. On the whole, the total number of the western flares is larger than that of eastern flares, but after normalization to the number of flares of every type, the difference between the fractions of western and eastern flares in all histograms practically disappears.

For the flares from the first three groups, we investigated the dependence of the minimum D_{st} index during a storm on the importance (i.e., the flux of X-ray emission or energy) of flares. This dependence is shown in the bottom panel of Fig. 5, where triangles, squares, and circles correspond to the most probable, probable, and unlikely sources, while open and solid symbols correspond to the to western and eastern flares, respectively. There is no dependence of the storm's intensity on the flare energy for all flares or for any subclass, although the flux of X-ray emission of the flares shown in the fig-

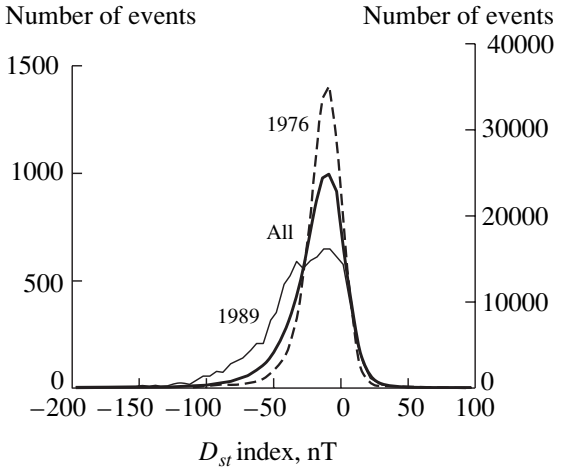

Fig. 3. Distributions of hourly averaged values of the D_{st} index for 1976–2000 (thick line, scale on the right), for the quiet year of 1976, and the disturbed year of 1989 (dashed and thin continuous lines, scale at the left).

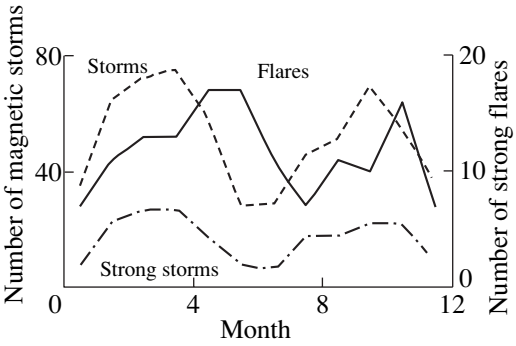

Fig. 4. Monthly distributions of the number of moderate and strong (dashed line) and strong (dot-dashed line) magnetic storms, and of strong solar flares (solid line) obtained by epoch superposition method for the period 1976–2000.

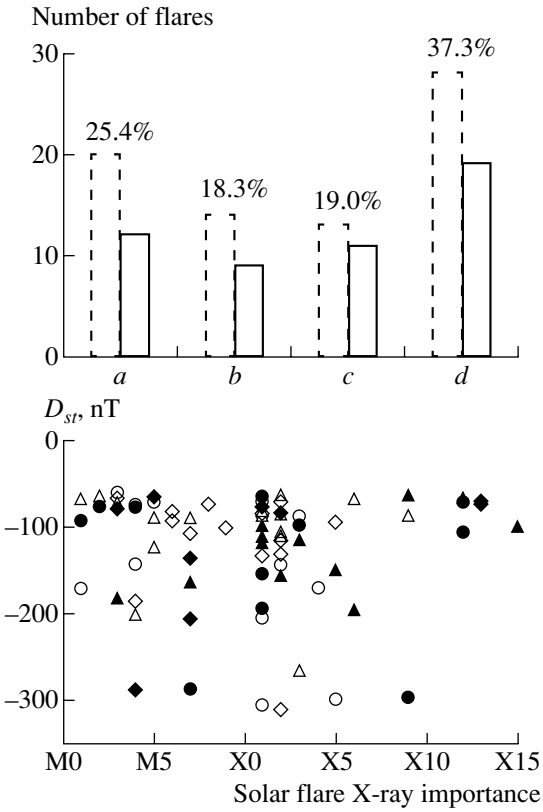

Fig. 5. Top panel: The number of western and eastern solar flares (dashed and solid lines, respectively), after which the most probable (*a*), probable (*b*), unlikely (*c*), and improbable (*d*) magnetic storms are observed. Below: The dependence of the minimum D_{st} index during magnetic storms on the importance (flux of energy) of solar flares. Open and solid symbols designate western and eastern flares; triangles, diamonds, and circles correspond to the events classified as *a*, *b*, and *c* on the top panel.

ure varies by 2.5 orders of magnitude. It is interesting that for the seven strongest flares of importance higher than X10, no storm with a D_{st} index less than –110 nT is observed, while for some flares of smaller importance, storms are observed with D_{st} indices as low as ~–300 nT.

In our previous paper [15], we analyzed the list of CMEs published in [16] and found out in 1996–1998 with the help of a coronagraph on the space observatory *SOHO*. They were also detected by the *WIND* spacecraft as MCs. The results of our analysis show that from these 28 CMEs, only 16 (57% of CME) have resulted in moderate and strong magnetic storms: 10 storms with D_{st} from –60 to –100 nT and 6 storms with D_{st} < –100 nT. In [17], based on the data taken from 1975 to 1983 by a photometer on *HELIOS* spacecraft, 38 CMEs were recorded moving along the Sun–Earth line. By estimating the CME propagation time from the Sun to the Earth and by an analysis of the magnetosphere disturbance according to the K_p index, it was obtained that one-half of CMEs (19) resulted in storms, 13 CMEs produced no storms, and no definite conclusion was possible for 6 CMEs. We can assume that some of the 6 CMEs were geoeffective after all. Therefore, the estimation of percentage of geoeffective CMEs as ~60%, obtained with two different samples for two different spacecraft, can be considered as sufficiently reliable.

4. RELATIONS OF STORMS WITH INTERPLANETARY SOURCES

When analyzing interplanetary sources, we did not analyze the whole database on SW. Instead, using the time of observation of magnetic storms, we searched for interplanetary disturbances that preceded and caused moderate and strong magnetospheric disturbances. Therefore, the geoefficiency of interplanetary disturbances discussed below has a somewhat different sense than that mentioned for solar flares in the previous section. The methods we used to identify SW types are described in detail in [4, 6, 7, 12]. The result of our analysis is given in Fig. 2, where various symbols show the identified types of SW streams, which could be interplanetary sources of strong storms (we do not present the results for moderate storms to avoid confusion in the figure). Measured interplanetary parameters are available only for about two-thirds (404 of 618) of the moderate and strong magnetic storms, but this allows us to estimate the distribution between different geoeffective SW types with sufficiently good statistics. The interplanetary sources of magnetic storms are (the figures in brackets are for moderate and strong storms, respectively): MCs in 33.2% (24.9 and 51.5%) of cases, CIRs in 30.2 (29.9 and 32.8%) of cases, ISs in 5.7 (6.9 and 3.7%) of cases, and other SW types in 30.9 (38.3 and 11.9%) of cases. Thus, in comparison with moderate storms, the fraction of strong storms from MCs increases from about one-fourth to one-half, the portion from CIRs remains at a level of about one-third, and the portion from ISs and other SW types decreases appreciably.

The analysis of behavior of the solar wind and IMF parameters (not shown here) for geoeffective events in interplanetary space confirms the well known fact that magnetospheric disturbances are produced by events in

Strong solar flares and corresponding interplanetary phenomena and minima of the D_{st} index

Solar flares						Correlation of events	Interplanetary phenomena				D_{st}, nT
no.	date	time, UT	importance, X-ray/optical	coord.	reg.		SW type	boundary	date	time, UT	
1	Apr. 30, 1976	21:14	X2/2B	S09W47	700	+	MC ?	IS	May 2, 1976	06	−107
2	Sept. 19, 1977	10:54	X2/3B	N08W58	889	+/–	No data		Sept. 21, 1977	10	−72
3	Nov. 22, 1977	10:06	X1/2N	N24W38	939	+	MC	IS	Nov. 25, 1977	12	−87
4	Feb. 13, 1978	02:55	M7/0B	N22W13	1001	+/–	No data		Feb. 15, 1978	11	−108
5	Apr. 11, 1978	13:53	X2/2B	N19W54	1057	+	MC ?	IS	Apr. 13, 1978	18	−80
6	Apr. 28, 1978	13:06	X5/4B	N22E41	1092	+	No data		May 1, 1978	23	−150
7	May 7, 1978	03:30	X2/2B	N22W64	1095	+/–	No data	Bz < –5	May 9, 1978	08	−132
8	May 31, 1978	10:09	M5/2B	N23W50	1129	–/+	?	IS	June 4, 1978	13	−71
9	June 22, 1978	17:09	M2/3B	N19E18	1164	–/+	No data	Bz < –5	June 26, 1978	10	−77
10	Sept. 23, 1978	10:23	X1/3B	N35W50	1294	–					
11	Nov. 10, 1978	00:42	M1/2N	N17E02	1385	–/+	IS	IS	Nov. 12, 1978	01	−93
12	Feb. 16, 1979	02:00	X2/2B	N15E48	1574	–					
13	June 5, 1979	05:29	X2/1N	N20E16	1781	–					
14	Aug. 18, 1979	14:16	X6/1B	N10E90	1943	–					
15	Sept. 14, 1979	08:02	X2/	N10E90	1994	+	?	Bz < –10	Sept. 18, 1979	00	−158
16	Nov. 15, 1979	16:39	M1/0B	N34W25	2110	–					
17	July 17, 1980	06:03	M3/1B	S12E06	2562	+/–	CIR ?	IS/LE	July 18, 1980	18	−80
18	Mar. 30, 1981	00:49	M3/2N	N13W74	2993	+/–	?	Bz < –5	Mar. 31, 1981	17	−67
19	Apr. 10, 1981	16:55	X2/3B	N09W40	3025	+/–	MC ?	IS	Apr. 12, 1981	15	−311
20	Apr. 24, 1981	14:00	X5/2B	N18W50	3049	+/–	MC ?	IS	Apr. 26, 1981	08	−95
21	May 8, 1981	22:52	M7/2B	N09E37	3099	+/–	CIR ?	IS/LE	May 10, 1981	21	−137
22	May 13, 1981	04:25	X1/3B	N11E58	3106	+	IS	IS	May 16, 1981	06	−119
23	July 20, 1981	13:29	M5/1B	S26W75	3204	+	IS	IS	July 23, 1981	07	−89
24	Aug. 7, 1981	19:16	M4/2B	S10E24	3257	–					
25	Oct. 7, 1981	23:08	X3/1B	S19E88	3390	+	MC ?	IS	Oct. 10, 1981	13	−116
26	Dec. 9, 1981	18:54	M5/3B	N12W16	3496	–					
27	Jan. 30, 1982	23:58	X1/3B	S13E19	3576	–					
28	June 3, 1982	11:46	X8/2B	S09E72	3763	–					
29	June 6, 1982	16:37	X12/3B	S11E26	3763	+	CIR ?	IS/LE	June 9, 1982	01	−66
30	July 9, 1982	07:42	X9/3B	N17E73	3804	+	MC ?	IS	July 11, 1982	12	−64
31	July 22, 1982	17:34	M4/0F	N29W86	3804	+/–	IS ?	IS	July 24, 1982	16	−75
32	Sept. 4, 1982	04:00	M4/3N	N11E30	3886	+/–	MC ?	IS	Sept. 5, 1982	21	−289
33	Nov. 22, 1982	18:28	M7/1N	S11W43	3994	–					
34	Nov. 26, 1982	02:53	X4/2B	S11W87	3994	–					
35	Dec. 7, 1982	23:54	X2/0B	S14W81	4007	–					
36	Dec. 15, 1982	02:02	X12/2B	S10E24	4026	–/+	No data	Bz < –5	Dec. 16, 1982	11	−106
37	Dec. 19, 1982	16:24	M9/2B	N10W75	4022	+/–	No data	Bz < –5	Dec. 21, 1982	05	−101
38	Dec. 25, 1982	07:52	X2/1B	S14E31	4033	–					
39	Feb. 3, 1983	06:19	X4/3B	S19W08	4077	–/+	No data		Feb. 4, 1983	22	−172
40	Feb. 17, 1984	23:01	X2/2B	0	0	–					
41	Mar. 14, 1984	03:34	M2/2B	S12W42	4433	–					
42	Apr. 25, 1984	00:05	X13/3B	S12E43	4474	+/–	No data		Apr. 26, 1984	20	−71

Table. (Contd.)

Solar flares						Correlation of events	Interplanetary phenomena				D_{st}, nT
no.	date	time, UT	importance, X-ray/optical	coord.	reg.		SW type	boundary	date	time, UT	
43	May 22, 1984	15:03	M6/2B	S09E24	4492	–					
44	May 31, 1984	11:42	M1	S09W90	4492	–					
45	Jan. 21, 1985	23:50	X4/2B	S08W38	4617	–					
46	Apr. 24, 1985	09:35	X1/3B	N06E27	4647	+	?	Bz < –5	Apr. 28, 1985	10	–98
47	July 9, 1985	02:04	M2/1B	S16W36	4671	+	No data	Bz < –5	July 11, 1985	18	–65
48	Feb. 6, 1986	06:25	X1/3B	S04W06	4711	–/+	MC ?	LE	Feb. 7, 1986	16	–307
49	Feb. 14, 1986	09:29	M6/1B	N01W76	4713	–					
50	May 4, 1986	10:07	M1	N06W90	4717	–/+	MC ?	LE	May 5, 1986	12	–94
51	Nov. 7, 1987	20:14	M1	N31W90	4875	–					
52	Jan. 2, 1988	21:45	X1/3B	S34W18	4912	+	No data		Jan. 6, 1988	19	–80
53	June 30, 1988	09:06	M9/2B	S16E22	5060	–					
54	Aug. 23, 1988	18:04	M2/EPL	N24E90	5125	–					
55	Oct. 12, 1988	05:11	X2/2N	S20W66	5175	–					
56	Nov. 7, 1988	11:05	M3/1N	S17W47	5212	–/+	?	Bz < –5	Nov. 8, 1988	14	–63
57	Nov. 13, 1988	23:09	M3/1N	S23W27	5227	–					
58	Dec. 15, 1988	05:05	X1/1N	N27E59	5278	+/–	?	Bz < –5	Dec. 17, 1988	05	–77
59	Jan. 4, 1989	17:53	M4/1N	S20W60	5303	–					
60	Mar. 6, 1989	14:05	X15/3B	N35E69	5395	+	IS	IS	Mar. 8, 1989	18	–100
61	Mar. 17, 1989	17:44	X6/2B	N33W60	5395	+	No data		Mar. 21, 1989	07	–68
62	Mar. 23, 1989	19:48	X1/3B	N18W28	5409	+/–	No data		Mar. 27, 1989	23	–87
63	Apr. 9, 1989	01:05	X3/4B	N35E29	5441	–/+	IS	IS	Apr. 13, 1989	22	–100
64	May 4, 1989	11:15	M5/2N	S20W36	5464	+	IS	IS	May 7, 1989	06	–90
65	May 22, 1989	00:37	M5/2B	S21E16	5497	+/–	No data		May 26, 1989	23	–66
66	June 29, 1989	21:27	M3/2B	N26W60	5555	–					
67	July 25, 1989	08:44	X2/2N	N25W84	5603	–					
68	Aug. 12, 1989	14:27	X2/2B	S16W37	5629	–/+	MC ?	IS	Aug. 14, 1989	00	–145
69	Sept. 3, 1989	14:32	X1/1B	S18E16	5669	–/+	No data		Sept. 4, 1989	06	–67
70	Sept. 12, 1989	08:14	M5/EPL	S18W79	5669	+	No data	IS	Sept. 15, 1989	02	–124
71	Sept. 29, 1989	11:33	X9/EPL	S26W90	5698	–					
72	Oct. 19, 1989	12:58	X13/4B	S27E10	5747	+/–	No data		Oct. 24, 1989	09	–74
73	Nov. 15, 1989	06:59	X3/3B	N11W26	5786	+	No data		Nov. 17, 1989	21	–266
74	Nov. 25, 1989	23:55	X1/2N	N30E05	5800	–					
75	Nov. 30, 1989	12:29	X2/3B	N26W59	5800	+	No data		Dec. 2, 1989	04	–85
76	Mar. 19, 1990	05:08	X1/2B	N31W43	5969	+/–	CIR ?	IS/LE	Mar. 21, 1990	00	–134
77	Mar. 28, 1990	07:51	M4/2N	S04W37	5988	+/–	CIR ?	IS/LE	Mar. 30, 1990	06	–187
78	Apr. 4, 1990	13:38	M7/0N	N22E72	6007	–					
79	Apr. 15, 1990	03:02	X1/2B	N32E57	6022	+	No data		Apr. 17, 1990	13	–113
80	May 21, 1990	22:19	X5/2B	N35W36	6063	–					
81	May 24, 1990	20:51	X9/1B	N33W78	6063	+	No data		May 27, 1990	08	–87
82	June 12, 1990	05:41	M6/2B	N10W33	6089	+/–	MC ?	IS	June 14, 1990	03	–93
83	July 30, 1990	07:36	M4/2B	N20E45	6180	–					
84	Jan. 31, 1991	02:30	X1/2B	S17W35	6469	–/+	No data		Feb. 1, 1991	23	–73

Table. (Contd.)

Solar flares						Correlation of events	Interplanetary phenomena				D_{st}, nT
no.	date	time, UT	importance, X-ray/optical	coord.	reg.		SW type	boundary	date	time, UT	
85	Feb. 25, 1991	08:19	X1/2N	S16W80	6497	–					
86	Mar. 22, 1991	22:47	X9/3B	S26E28	6555	–/+	No data		Mar. 24, 1991	10	–298
87	Apr. 2, 1991	23:27	M6/3B	N14W00	6562	+/–	No data		Apr. 4, 1991	20	–83
88	May 13, 1991	01:44	M8	S09W90	6615	+/–	No data		May 14, 1991	17	–74
89	June 4, 1991	03:52	X12/3B	N30E70	6659	–/+	No data		June 9, 1991	19	–73
90	June 15, 1991	08:21	X12/3B	N33W69	6659	+	IS ?	IS	June 17, 1991	11	–70
91	June 28, 1991	06:26	M6	N30E85	6703	–					
92	July 7, 1991	02:23	X1/2B	N26E03	6703	–/+	CIR ?	IS/LE	July 8, 1991	18	–194
93	July 10, 1991	12:28	M3/2N	S22E34	6718	+	No data		July 13, 1991	15	–183
94	Aug. 25, 1991	01:15	X2/2B	N25E64	6805	–					
95	Sept. 29, 1991	15:33	M7/4B	S21E32	6853	+	No data		Oct. 2, 1991	03	–164
96	Oct. 27, 1991	05:48	X6/3B	S13E15	6891	+	MC ?	IS	Oct. 30, 1991	23	–196
97	Oct. 30, 1991	06:34	X2/3B	S08W25	6891	–					
98	Feb. 6, 1992	10:48	M4/2B	S13W10	7042	+	MC ?	IS	Feb. 6, 1992	15	–201
99	Mar. 15, 1992	01:54	M7/3B	S14E29	7100	–					
100	May 8, 1992	15:46	M7/4B	S26E07	7154	–/+	No data	IS	May 9, 1992	19	–288
101	June 25, 1992	20:14	X3/2B	N09W67	7205	–/+	No data		July 1, 1992	03	–89
102	Aug. 3, 1992	07:06	M4/1N	S09E68	7248	–/+	MC ?	IS	Aug. 4, 1992	14	–77
103	Oct. 30, 1992	18:16	X1/2B	S22W61	7321	+	No data		Nov. 2, 1992	06	–70
104	Mar. 12, 1993	18:15	M7/3B	S00W51	7440	+	No data	IS	Mar. 15, 1993	16	–90
105	Feb. 20, 1994	01:41	M4/3B	N09W02	7671	–/+	MC ?		Feb. 21, 1994	09	–144
106	Oct. 19, 1994	21:27	M3/1F	N12W24	7790	+	No data		Oct. 23, 1994	06	–71
107	Oct. 20, 1995	06:07	M1/0F	S09W55	7912	–					
108	Nov. 4, 1997	05:58	X2/2B	S14W33	8100	+	MC	IS	Nov. 6, 1997	22	–110
109	Apr. 20, 1998	10:21	M1/EPL	S43W90	8194	+	CIR	IS/LE	Apr. 23, 1998	18	–69
110	May 2, 1998	13:42	X1/3B	S15W15	8210	–/+	MC	IS	May 4, 1998	03	–205
111	May 6, 1998	08:09	X2/1N	S11W65	8210	+	?	Bz < –5	May 9, 1998	15	–63
112	Aug. 24, 1998	22:12	X1/3B	N30E07	8307	–/+	CIR	IS/LE	Aug. 26, 1998	07	–155
113	Sept. 23, 1998	07:13	M7/3B	N18E09	8340	+/–	MC	IS	Sept. 24, 1998	23	–207
114	Sept. 30, 1998	13:50	M2/2N	N23W81	8340	–					
115	Jan. 20, 1999	20:04	M5	N27E90	0	–					
116	May 3, 1999	06:02	M4/2N	N15E32	8525	–					
117	June 4, 1999	07:03	M3/2B	N17W69	8552	–					
118	Feb. 17, 2000	20:35	M1/2N	S29E07	8872	–					
119	June 6, 2000	15:25	X2/3B	N20E18	9026	+/–	CIR	IS/LE	June 8, 2000	09	–85
120	June 10, 2000	17:02	M5/3B	N22W38	9026	–					
121	July 14, 2000	10:24	X5/3B	N22W07	9077	–/+	CIR	LE	July 15, 2000	15	–300
122	July 22, 2000	11:34	M3/2N	N14W56	9085	–					
123	Sept. 12, 2000	12:13	M1/2N	S17W09	Filam	–/+	CIR	IS/LE	Sept. 17, 2000	16	–172
124	Oct. 16, 2000	07:28	M2	N04W90	9182 ?	–					
125	Nov. 8, 2000	23:28	M7/mu	N00–10 W75–80	9212, 13, 18	–					
126	Nov. 24, 2000	05:02	X2/3B	N20W05	9236	+/–	CIR	LE	Nov. 29, 2000	05	–117

Note: LE is leading edge, + means a good correlation (falling within a window of 2–4 days), +/– is probable correlation (windows 1.5–2 and 4–5 days), –/+ is unlikely correlation (windows 1–1.5 and 5–6 days), and – is no correlation at all.

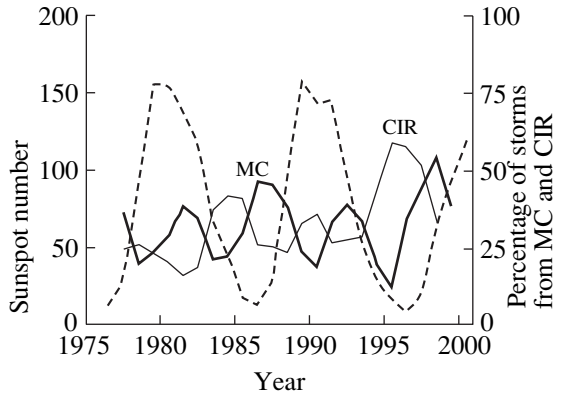

Fig. 6. Time variation of the fraction of magnetic storms generated by MC (thin line) and by CIR (thick line). The dashed line represents the sunspot number (scale on the left).

which a large negative (southward) IMF component is observed for a sufficiently long time. It is precisely this situation that is most frequently registered in MC, CIR, and after IS passages. One can explain this as follows. If a southward IMF component was in originally undisturbed solar wind, then as a result of dynamic processes during the motion of MC, CIR, and IS, compression takes place, and all IMF components increase in the region of compression, including the IMF component parallel to the terrestrial magnetic dipole.

In our previous paper [18], we showed that during the growth phase of the 23rd solar cycle, initially, the number of the storms generated by MC increases, then the number of these storms decreases, and the number of CIR storms increases. Here, we have the possibility to investigate the cycle variation of fractions of storms from MC and CIR over more than two solar cycles. For this purpose, we found for every year the ratio of the total number of moderate and strong storms from MC and CIR, respectively, to the number of storms, for which it was possible to determine SW type. These results are presented in Fig 6. Since the mean number of storms per year is not large, especially in the minimum of a cycle, we have smoothed these ratios by a sliding average over three points to remove high-frequency fluctuations due to small statistics. Figure 6 confirms the conclusion made earlier in [18] for the beginning of a growth phase. However, it shows that the curves for MC and CIR have two maxima during a solar cycle.

5. DISCUSSION OF RESULTS AND CONCLUSIONS

The analysis of 25-year series of observations of the Sun, the solar wind, and magnetospheric disturbances has confirmed some of the effects found earlier, such as the correlation of the sunspot number with the number of solar flares and with the number of magnetic storms on the Earth, as well as the Russell–McPherron effect [14] (i.e., preferred generation of magnetic storms in spring and autumn months). However, the data presented on the connections between solar, interplanetary, and magnetospheric disturbances also contain new results.

Let us consider in more detail the connection of strong solar flares and CMEs with moderate and strong magnetic storms. First, for the sake of simplicity, we assume that among the probable and unlikely flares (see Section 3), the numbers of events, which have both resulted and not resulted in magnetic storms, is distributed as 3 : 1 and 1 : 3, respectively. Then, the numbers of geoeffective and ineffective strong solar flares are 44 and 56%, respectively. For CME, one can, apparently, put these numbers equal to 60 and 40%, i.e., geoefficiency of CME is higher by ~30%. Let us consider to what extent these conclusions are statistically significant. As was already noted above, the period of moderate and strong magnetic storms varies over the solar cycle from ~6.8 days in disturbed years up to ~45 days in quiet years with a mean value of ~15 days. Since we are interested in years when the Sun was active, it is reasonable to take a value of 8–10 days for further analysis. Since the time lag between a solar event and a storm is usually taken to be equal to ~3.5 days (a window of 1.5 to 5 days), it is possible to estimate the probability of observing a storm (as the ratio of the window duration to the average period between storms), if both a solar event and a storm occur randomly. According to this estimate, the correlation between the solar and ground phenomena will be observed in 35–44% of cases even at a random distribution of these phenomena. Therefore, the obtained geoefficiency of strong solar flares can be in part or completely ascribed to random processes. This is supported by the absence of a correlation between the importance of a solar flare and the magnetic storm intensity (see Fig. 5). The geoefficiency of CME is higher than that of solar flares and higher than the obtained threshold for random processes, and this suggests that the obtained connections between CME and geomagnetic disturbances are real.

Note that the estimations of the geoefficiency of flares and CME obtained here are also too low to predict "space weather," since the percentage of false predictions is very large. The only way to increase the efficiency of prediction is to select solar events on the basis of additional parameters, resulting in the rejection of events that do not have sufficient geoefficiency. Accordingly, the method of determining the magnetic field orientation in the ejected plasma using its initial configuration in the solar atmosphere [4] is very promising. It is also important to predict the trajectory and dynamics of a geoeffective solar phenomenon in interplanetary space first, to estimate the probability of its arrival in the Earth's magnetosphere, and second, to predict the time of propagation from the Sun to the Earth with sufficient accuracy.

In contrast to the analysis of solar sources of magnetic storms, where the lists of events on the Sun were taken as a basis, only the intervals of the solar wind corresponding to the moderate and strong magnetic storms were used in the analysis of interplanetary sources of storms. Therefore, the meaning of the term "geoeffective event" is somewhat different (see Section 4). The main interplanetary sources of moderate and strong magnetic storms are MC and CIR, each of which are responsible for about one-third of all geoeffective SW types. In comparison with moderate storms, the fraction of strong storms from MC increases and reaches one-half of all geoeffective SW types, the number of storms from CIR practically does not change, and the fraction of storms from other SW types significantly decreases. Our results on the correlation of magnetic storms and MCs agree well with [6]; although, in contrast to our paper, MCs were determined in that research on the basis of counterstreaming electrons and storms were determined by the K_p index. Our dependence of the fraction of magnetic storms generated by MCs (as well as by CIRs) on the solar cycle has two maxima in a cycle. The curves for storms from MCs and from CIRs change in an antiphase, as could be expected, because the sum of fractions of storms from MCs and CIRs should be a constant close to two-thirds, with one-third made up by other SW types. This result is consistent with observations in 1979–1988 of the distribution of magnetic storms from streams such as MCs and CIRs in the SW at a distance of 0.7 AU on the *PVO* spacecraft [19]. In this paper, it was found that MC is more geoeffective in the maximum and CIR is more effective in the minimum of the solar cycle. This is true if our results (see Fig. 6) in the minimum of cycles from 1986 to 1988 are ignored. In general, the dependence obtained by us has a more complicated character over a longer period than in [19].

Irrespective of the SW type, which results in a magnetospheric storm, the southward IMF component (in the GSM system of coordinates) is almost always observed in interplanetary space, with a value of –5 to –15 nT and a duration of 1–3 h and more. Intervals of southward IMF component are observed more frequently (1) after shock waves, both isolated and connected with MC or CIR, (2) in the region of compression directly ahead of an MC body and in CIR, and (3) in the MC body. Although the models predicting geomagnetic disturbances on the basis of SW and IMF measurements in real time in the L1 libration point (for example, on the *Wind* (1994) and *ACE* (1997) spacecraft) have a short-term character (about half an hour), their reliability satisfies practical criteria [5]. At present, no reliable long-term (more than 1 day) techniques of predicting magnetospheric disturbances exist. For such predictions, it is required to begin the forecast with an analysis of phenomena on the Sun and, as we have already noted above, the reliability of available techniques for estimation of the geoeffective solar phenomena is insufficient. There are two main causes of this. First, the problem has a pronounced multidisciplinary character, and the joint efforts of scientists of different specialties are required to solve it. The second reason is our limited knowledge about specific physical mechanisms of many observed phenomena, including those that provide the transfer of energy between separate parts of a chain. In these conditions, special attention should be paid to the statistical methods that quantitatively describe observed relationships between the phenomena on the Sun, in interplanetary space, and in the Earth's magnetosphere. It is not uncommon that some *hypotheses* about the connections between separate phenomena are then considered as proved *facts* in related scientific research, and on their basis, new *hypotheses* are constructed. In our opinion, insufficient distinction between facts and hypotheses is an appreciable retarding factor for progress in investigating the solar–terrestrial links.

ACKNOWLEDGMENTS

The authors are grateful to the international scientific data centers SEC NOAA, NSSDC/GSFC NASA, and WDC-C2. We also thank L.M. Zelenyi, A.A. Petrukovich, and G.N. Zastenker for their attention, help, and useful discussions of this research. The work is supported in part by the Russian Foundation for Basic Research, project no. 01-02-16128, and by INTAS, grant 99-0078.

REFERENCES

1. *Solar Drivers of Interplanetary and Terrestrial Disturbances*, Balasubramaniam, K.S., Keil, S.L., and Smartt, R.N., Eds., ASP Conference Series, 1996.
2. Webb, D.F., Coronal Mass Ejections: The Key to Major Interplanetary and Geomagnetic Disturbances, *Rev. Geophys. Suppl.*, 1995, p. 577.
3. Gonzalez, W.D., Tsurutani, B.T., and Clua de Gonzalez, A.L., Interplanetary Origin of Geomagnetic Storms, *Space Sci. Rev.*, 1999, vol. 88, p. 529.
4. Crooker, N.U., Solar and Heliospheric Geoeffective Disturbances, *J. of Atmospheric and Solar-Terrestrial Physics*, 2000, vol. 62, p. 1071.
5. Petrukovich, A.A. and Klimov, S.I., The Use of Solar Wind Measurements for the Analysis and Prediction of Geomagnetic Activity, *Kosm. Issled.*, 2000, vol. 38, no. 5, pp. 463–468.
6. Gosling, J.T., McComas, D.J., Phillips, J.L., and Bame, S.J., Geomagnetic Activity Associated with Earth Passage of Interplanetary Shock Disturbances and Coronal Mass Ejections, *J. Geophys. Res.*, 1991, vol. 96, p. 7831.
7. Gosling, J.T. and Pizzo, V.J., Formation and Evolution of Corotating Interaction Regions and Their Three-Dimensional Structure, *Space Sci. Rev.*, 1999, vol. 89, p. 21.
8. Miroshnichenko, L.I., Solar–Terrestrial Links, in *Fizika kosmosa: malen'kaya entsiklopediya* (Physics of Space: A Small Encyclopedia), Syunyaev, R.A., Ed., Moscow: Sovetskaya Entsiklopediya, 1986, p. 629.

9. Gosling, J.T., The Solar Flare Myth, *J. Geophys. Res.*, 1993, vol. 98, p. 18937.
10. Webb, D.F., Cliver, E.W., Crooker, N.U., *et al.*, Relationship of Halo Coronal Mass Ejections, Magnetic Clouds, and Magnetic Storms, *J. Geophys. Res.*, 2000, vol. 105, p. 7491.
11. Burlaga, L.F.E., *Magnetic Clouds*, vol. 2 of *Physics of the Inner Magnetosphere*, Schwenn, R. and Marsch, E., Eds., New York: Springer, 1991.
12. Burlaga, L., Fitzenreiter, R., Lepping, R., *et al.*, A Magnetic Cloud Containing Prominence Material: January 1997, *J. Geophys. Res.*, 1998, vol. 103, p. 277.
13. Shodhan, S., Crooker, N.U., Kahler, S.W., *et al.*, Counterstreaming Electrons in Magnetic Clouds, *J. Geophys. Res.*, 2000, vol. 105, p. 27261.
14. Russell, C.T. and McPherron, R.L., Semiannual Variation of Geomagnetic Activity, *J. Geophys. Res.*, 1973, vol. 78, p. 241.
15. Yermolaev, Yu.I., Zastenker, G.N., and Nikolaeva, N.S., The Earth's Magnetosphere Response to Solar Wind Events according to the INTERBALL Project Data, *Kosm. Issled.*, 2000, vol. 38, no. 6, pp. 563–576.
16. Gopalswamy, N., Lara, A., and Lepping, R.P., *et al.*, Interplanetary Acceleration of Coronall Mass Ejections, *Geophys. Res. Lett.*, 2000, vol. 27, p. 145.
17. Webb, D.F., Geomagnetic Storms and Heliospheric CMEs as Viewed from HELIOS, in *Solar Drivers of Interplanetary and Terrestrial Disturbances*, ASP Conference Series, 1996, vol. 95, p. 167.
18. Yermolaev, Yu.I., Strong Geomagnetic Disturbances and Their Correlation with Interplanetary Phenomena during the Operation of the INTERBALL Project Satellites, *Kosm. Issled.*, 2001, vol. 39, no. 3, p. 324–331.
19. Lindsay, G.M., Russell, C.T., and Luhman, J.G., Coronal Mass Ejection and Stream Interaction Region Characteristics and Their Potential Geomagnetic Effectiveness, *J. Geophys. Res.*, 1995, vol. 100, p. 16999.